The American Journal of Pathology, Vol. 170, No. 1, January 2007

DOI: 10.2353/ajpath.2007.060806

Cell Injury, Repair, Aging and Apoptosis

Aggregated Myocilin Induces Russell Bodies and Causes Apoptosis

Implications for the Pathogenesis of Myocilin-Caused Primary Open-Angle Glaucoma

Gary Hin-Fai Yam, Katarina Gaplovska-Kysela, Christian Zuber, and Jürgen Roth

From the Department of Pathology, Division of Cell and Molecular Pathology, University of Zurich, Zurich, Switzerland

Primary open-angle glaucoma with elevated intraocular pressure is a leading cause of blindness worldwide. Mutations of myocilin are known to play a critical role in the manifestation of the disease. Misfolded mutant myocilin forms secretion-incompetent intracellular aggregates. The block of myocilin secretion was proposed to alter the extracellular matrix environment of the trabecular meshwork, with subsequent impediment of aqueous humor outflow leading to elevated intraocular pressure. However, the molecular pathogenesis of myocilin-caused glaucoma is poorly defined. In this study, we show that heteromeric complexes composed of wild-type and mutant myocilin were retained in the rough endoplasmic reticulum, aggregating to form inclusion bodies typical of Russell bodies. The presence of myocilin aggregates induced the unfolded protein response proteins BiP and phosphorylated endoplasmic reticulum-localized eukaryotic initiation factor-2α kinase (PERK) with the subsequent activation of caspases 12 and 3 and expression of C/EBP homologous protein (CHOP)/GADD153, leading to apoptosis. Our findings identify endoplasmic reticulum stress-induced apoptosis as a pathway to explain the reduction of trabecular meshwork cells in patients with myocilin-caused glaucoma. As a consequence, the phagocytotic capacity of the remaining trabecular meshwork cell population would be insufficient for effective cleaning of aqueous humor, constituting a major pathogenetic factor for the development of increased intraocular pressure in primary open-angle glaucoma. ***(Am J Pathol 2007, 170:100–109; DOI: 10.2353/ajpath.2007.060806)***

Glaucoma is a heterogeneous group of optic neuropathies characterized by a progressive degeneration of the optic nerve resulting in an irreversible loss of vision.[1] After age-related macular degeneration, it is the second leading cause of severe vision loss or blindness.[2] It is expected that ~4% of the world population older than the age of 40 will develop glaucoma. Primary open-angle glaucoma (POAG) is the most common form of the disease.[2] In most cases of POAG, the aqueous humor outflow from the anterior eye chamber is impeded, resulting in an elevated intraocular pressure (IOP) and causing ganglion cell death in the neural retina.[3,4] Hence, impaired outflow drainage along the trabecular meshwork (TM) and Schlemm's canal seems to be central in the pathogenesis of POAG.[3,4]

The flow of aqueous humor is important in providing nutritive support for the avascular anterior eye tissues, such as cornea and lens. The aqueous humor is constitutively produced by the ciliary body, enters the anterior eye chamber, and exits it through the TM, a reticulated network of cell-lined extracellular matrix located at the junction of cornea and iris, enters the Schlemm's canal, and finally the venous circulation.[5] The cells of the TM seem to play a regulatory role in humor outflow. TM cells synthesize and release glycosaminoglycans, glycoproteins, and fibrillar materials[6] and are active as phagocytes.[7] By phagocytosing particulate matter of various origins, TM cells help to maintain the structural and functional integrity of the TM drainage pathway.

Supported by the Velux Foundation (Zurich), the Kamillo Eisner Foundation (Hergiswil), and the Canton of Zurich.

Accepted for publication October 12, 2006.

Current address of G.H.-F.Y.: Department of Ophthalmology and Visual Sciences, The Chinese University of Hong Kong, Hong Kong, People's Republic of China.

Address reprint requests to Jürgen Roth, M.D., Ph.D., Division of Cell and Molecular Pathology, Department of Pathology, University of Zurich, CH-8091 Zurich, Switzerland. E-mail: juergen.roth@usz.ch.

Different organotypic and cell culture models have been used to investigate the role of TM cells in the outflow drainage. Disruption of the actin cytoskeleton by inhibition of Rho kinase in organ culture of anterior eye segment reduces the focal adhesion of TM cells and increases aqueous humor outflow.[8] Expression of recombinant Hep II domain of fibronectin has also found to increase the outflow.[9] In contrast, dexamethasone-induced actin cross-linking reduces aqueous humor outflow in a perfusion model of isolated anterior segment.[10] These data point to a role of cell-extracellular matrix interactions in the outflow drainage. On the other hand, mutations of the myocilin (*MYOC*) gene have been found in most families with juvenile-onset POAG and in ~4% of patients with adult-onset POAG. *MYOC* was the first identified glaucoma-causing gene,[11] and the majority of patients with *MYOC* mutations suffer from high IOP.[12] MYOC is synthesized and secreted by TM cells[13–16] and has been found to be associated with different microfibrillar structures and with sheath-derived plaque material in the TM.[17,18] A recent functional analysis has shown the importance of the olfactomedin-homology domain of MYOC for its secretion and that of the amino-terminal coiled-coil regions for the interactions of MYOC with extracellular matrix components.[19]

The molecular pathogenesis of MYOC-caused POAG is still poorly defined.[20] Absence[21] or overexpression[22] of wild-type (WT) MYOC in transgenic mice has been shown not to be critical for the development of POAG. However, many glaucoma-causing mutant MYOCs have been found to be misfolded and to form detergent-resistant, secretion-incompetent aggregates.[19,23–27] The secretion block of POAG-causing mutant MYOCs could be overcome by lowering the cell culture temperature from 37 to 30°C, a condition known to improve protein folding.[17,19] Increasing evidence suggests that mutant MYOC acts by a pathological gain-of-function mechanism.[21,28,29] In agreement with this, several missense and truncated mutant MYOCs have been shown to interact with WT MYOCs to form heteromeric protein aggregates resulting in a block of secretion of WT MYOCs as well.[25,30,31]

MYOC-secreting TM cells are phagocytotically active and keep the outflow drainage along the TM clean of deposits of particulate matter of various origin.[7,32–34] We reasoned that a disturbance of the phagocytotic capacity of the TM cell population could be a pathogenetic factor in the development of MYOC-caused POAG. This is supported by electron microscopic findings of thickened trabeculae and the accumulation of sheath-derived plaques and of melanin.[3,17,35–39] Furthermore, a reduction of the number of TM cells has been observed in glaucoma patients.[36,40] Although mutant MYOC singly expressed in different cell types has been shown to be cytotoxic,[25,26,30] its mechanism of action remains elusive. The possible cytotoxicity of heteromeric mutant/WT MYOC complexes whose formation is the basis for the pathological gain-of-function mechanism has not been addressed yet.

In the present study, we provide evidence for a link between the formation of heteromeric mutant/WT MYOC aggregates, endoplasmic reticulum (ER) stress, and apoptosis. In a cell culture system, we demonstrate Russell body formation by ER-retained heteromeric mutant/WT MYOC aggregates, which induce ER stress and lead to apoptosis. This supports the proposal that the phagocytotic capacity of the reduced TM cell population is insufficient for effective cleaning of the TM. This may represent an important pathogenetic factor for the development of increased IOP in patients with POAG.

Materials and Methods

Cells and Reagents

Chinese hamster ovary (CHO)-K1 and human embryonic kidney (HEK) 293 cells were purchased from American Type Culture Collection (Manassas, VA) and immortalized human TM (HTM) cells[41] were kindly provided by T.D. Nguyen (San Francisco, CA). MYOC mRNA or MYOC protein was undetectable in the human TM cells by reverse transcriptase-polymerase chain reaction (RT-PCR) and Western blotting, respectively (data not shown). Culture media, Lipofectamine 2000, protein A Dynabeads, fetal bovine serum, normal goat serum, and Geneticin 418 were from Invitrogen (Basel, Switzerland), Fugene 6 and protease inhibitor cocktail from Roche Diagnostics (Rotkreuz, Switzerland), expression vectors pEGFP-N_3 from Clontech (Basel, Switzerland), QuikChange II site-directed mutagenesis kit from Stratagene (La Jolla, CA), and p3xFLAG-myc-CMV-25 from Sigma (Buchs, Switzerland). Oligonucleotides were synthesized by MicroSynth (Balgach, Switzerland). MG132 was from Calbiochem (La Jolla, CA), enhanced chemiluminescence Western blotting detection kit from Amersham Biosciences (Buckinghamshire, UK), [^{35}S]cysteine and [^{35}S]methionine from Anawa (Wangen, Switzerland), and EN^{3}hance from Perkin-Elmer (Boston, MA). Mouse monoclonal antibodies against the ER chaperone BiP (BD Biosciences, San Jose, CA), the pre-Golgi intermediate marker ERGIC-53 (a gift from H.P. Hauri, Biozentrum, University of Basel, Basel, Switzerland), GAPDH (Ambion, Austin, TX), and β-actin (Sigma) and rabbit polyclonal antibodies against green fluorescent protein (GFP; Molecular Probes, Eugene, OR), FLAG (Sigma), phosphorylated ER-localized eukaryotic initiation factor (eIF)-2α kinase (PERK; Santa Cruz Biotechnology Inc., Santa Cruz, CA), C/EBP homologous protein (CHOP)/GADD153 (Alexis, Lausen, Switzerland), caspase 3 (Upstate, Lake Placid, NY), and caspase 12 (ProSci, Poway, CA) were used. Alexa 488-conjugated goat anti-rabbit Ig antibody (Molecular Probes), red X-conjugated Fab fragments of goat anti-mouse Ig or anti-rabbit Ig (Jackson ImmunoResearch, West Grove, PA), and horseradish peroxidase-conjugated donkey anti-rabbit Ig or sheep anti-mouse Ig antibodies (Amersham Biosciences) were used. Bovine serum albumin, Triton X-100 and diaminobenzidine tetrahydrochloride (DAB) were from Sigma, glutaraldehyde and osmium tetroxide from EMD (Gibbstown, NJ), formaldehyde from Merck (Basel, Switzerland), and Epon-Araldite from Fluka (Buchs, Switzerland).

All other chemicals were of analytical grade and from Sigma.

Plasmids and Mutagenesis

Human full-length MYOC cDNA was obtained from human skeletal muscle and cloned into the expression vector pEGFP-N_3 and p3xFLAG-myc-CMV-25 to generate the constructs pEGFP-$MYOC^{WT}$ and pFLAG-$MYOC^{WT}$, respectively. Mutations in *MYOC* cDNA were introduced by a PCR-based method using QuikChange II site-directed mutagenesis kit and specific primers. The sense primer sequences with the altered bases underlined for C245Y MYOC were 5′-GAGTGGAGAGGGAGACACCGGATATGGAGAACTAGTTTGGGTAGG-3′; for G364V MYOC: GAAGGAAATCCCTGGAGCTGTCTACCACGGACAGTTCCCG-3′; for P370L MYOC: 5′-CTGGCTACCACGGACAGTTCCTGTATTCTTGGGGTGGCTACACG-3′; for R422C MYOC: 5′-CAAACCTGGGAGACAAACATCTGTAAGCAGTCAGTCGCCAATGCC-3′; for R422H MYOC: 5′-CAAACCTGGGAGACAAACATCCATAAGCAGTCAGTCGCCAATGCC-3′; and for Y437H MYOC: 5′-CATCATCTGTGGCACCTTGCACACCGTCAGCAGCTACACC-3′. The correctness of all constructs was verified by direct sequencing.

Cell Culture and Transfection

CHO-K1 and HEK293 cells were cultured in minimal essential medium supplemented with 10% fetal bovine serum, 110 μg/ml sodium pyruvate, and antibiotics. HTM cells were grown in Dulbecco's modified Eagle's medium (1 mg/ml D-glucose) supplemented with fetal bovine serum, sodium pyruvate, and antibiotics. Cells at ~50% confluence were transfected with plasmids containing WT or different mutant *MYOC* cDNAs by Fugene 6 or Lipofectamine 2000 according to the manufacturer's protocol with a ratio of 3 μl of transfection reagent per μg of DNA. For stable MYOC expression, the cells were selected with 100 μg/ml Geneticin 418 in culture medium for 10 days, and cells with suitable MYOC expression level were clonally expanded. For double MYOC expression, cells stably expressing MYOC-GFP fusion protein were transiently transfected with pFLAG-$MYOC^{WT}$ and analyzed within 5 days.

Monitoring Myocilin Secretion

Cells were incubated with media containing 25 μCi/ml [^{35}S]cysteine and [^{35}S]methionine for 24 hours. Culture media were collected and centrifuged to remove cell debris. The supernatant was immunoprecipitated with polyclonal antibodies against FLAG bound to protein A Dynabeads. Immunoprecipitated proteins were denatured in sodium dodecyl sulfate (SDS) sample buffer containing 20% β-mercaptoethanol and resolved by 10% SDS-polyacrylamide gel electrophoresis (PAGE). The gel was treated with EN^{3}hance, and radioactivity was detected by a Bio-Imaging analyzer (BAS-1800II; Fujifilm, Wayne, NJ).

Analysis of Triton X-100-Insoluble MYOC

Cells were washed twice with ice-cold phosphate-buffered saline (PBS) and lysed in buffer containing 100 mmol/L Tris-HCl (pH 7.4), 3 mmol/L EGTA, 5 mmol/L $MgCl_2$, 0.5% Triton X-100, protease inhibitor cocktail, and 1 mmol/L phenylmethyl sulfonyl fluoride for 2 minutes on ice.[23] After centrifugation, the pellet containing Triton X-100-insoluble proteins was washed with ice-cold PBS twice, sonicated, and denatured in SDS sample buffer containing 9 mol/L urea. Triton X-100-insoluble proteins from samples equivalent to 2×10^5 cells were analyzed by 10% SDS-PAGE and Western blotting using antibodies against GFP, FLAG, or β-actin, respectively, and appropriate horseradish peroxidase-conjugated secondary antibodies. The signals were detected by enhanced chemiluminescence.

Monitoring Myocilin Degradation

MYOC-GFP-expressing cells grown to ~70% confluence were incubated in cysteine- and methionine-free Dulbecco's modified Eagle's medium containing 10% dialyzed fetal bovine serum for 5 minutes at 37°C. For metabolic labeling, the cells were incubated in fresh medium containing 100 μCi/ml [^{35}S]cysteine and [^{35}S]methionine for 8 minutes. After two rinses with PBS, the cells were cultured in fresh medium supplemented with 1 mmol/L nonradioactive cysteine and methionine in the presence or not of 10 μmol/L MG132 for periods ranging from 1 to 8 hours. The cells were washed with ice-cold PBS and lysed in radioimmunoprecipitation assay (RIPA) buffer containing 50 mmol/L Tris-HCl (pH 7.4), 150 mmol/L NaCl, 1% Nonidet P-40, 0.25% sodium deoxycholate, protease inhibitor cocktail, and 1 mmol/L phenylmethyl sulfonyl fluoride for 30 minutes on ice. After centrifugation, the supernatant was immunoprecipitated for GFP and analyzed.

Western Blotting

Cells expressing WT or co-expressing mutant MYOC-GFP and FLAG-WT MYOC were lysed in RIPA buffer. To study PERK expression, phosphatase inhibitors (1 mmol/L sodium fluoride, 1 mmol/L sodium orthovanadate, and 10 mmol/L sodium diphosphate) were added to the RIPA buffer. After centrifugation, the supernatant was denatured in SDS sample buffer containing 50 mmol/L dithiothreitol and samples (20 μg) were resolved by 8 or 12% SDS-PAGE followed by incubation with antibodies against BiP, PERK, caspase 12, CHOP/GADD153, caspase 3, FLAG, GFP, or GAPDH and appropriate horseradish peroxidase-conjugated secondary antibodies. Signals were detected by enhanced chemiluminescence.

Electron Microscopy

For conventional transmission electron microscopy, cells were fixed *in situ* with 3% glutaraldehyde followed by 1%

osmium tetroxide and embedded in Epon-Araldite according to standard protocol. Ultrathin sections were prepared using an Ultracut S ultramicrotome (Leica, Wetzlar, Germany), contrasted with 1% uranyl acetate and lead citrate and examined with an EM912 AB transmission electron microscope (Zeiss, Oberkochen, Germany).

Subcellular distribution of MYOC in mutant/WT MYOC-expressing HEK293 cells was analyzed by pre-embedding immunoperoxidase electron microscopy.[42] In brief, cells grown on glass coverslips were fixed with freshly prepared 2% formaldehyde in phosphate buffer (pH 7.4, 0.15 mol/L NaCl) for 10 minutes at 37°C, permeabilized with 0.05% saponin in PBS containing 1.5% normal goat serum and 0.1% bovine serum albumin for 10 minutes, incubated with polyclonal antibody to FLAG followed by horseradish peroxidase-conjugated secondary antibody, both diluted in PBS containing 1% bovine serum albumin and 0.05% saponin. Afterward, cells were washed in 0.1 mol/L cacodylate buffer (pH 7.4), postfixed in 2% buffered glutaraldehyde for 1 hour. Peroxidase activity was revealed by the DAB reaction. DAB (0.2%) was dissolved in 50 mmol/L Tris-HCl, pH 7.4, containing 7.5% sucrose to which H_2O_2 was added (final concentration, 0.002%). Coverslips were incubated with the DAB solution for 17 minutes. After washing, samples were fixed with 1% reduced osmium tetroxide in cacodylate buffer, dehydrated in a series of graded ethanol, and embedded *in situ* in Epon-Araldite. Ultrathin sections were prepared parallel to the plane of the cell monolayer, contrasted, and examined by transmission electron microscopy.

Immunofluorescence

HEK293 cells co-expressing WT or mutant MYOC-GFP and FLAG-WT MYOC were grown on glass coverslips, fixed with freshly prepared 2% formaldehyde, permeabilized with 0.05% saponin, and processed for double immunofluorescence as described previously.[43] To detect MYOC and ERGIC-53, polyclonal anti-FLAG antibody and monoclonal anti-ERGIC-53 antibody followed by Alexa 488-conjugated goat anti-rabbit Ig antibody and red X-conjugated Fab fragments of goat anti-mouse Ig antibody were used, respectively. Samples were examined with a CLSM SP2 confocal laser-scanning microscope (Leica) using a ×63 (n.a., 1.4) blue-corrected objective.

To measure the apoptosis rate in mutant/WT MYOC-expressing cells, formaldehyde-fixed cells were immunostained with antibody against FLAG followed by red X-conjugated secondary antibody. Nuclei were stained with Hoechst 33250 (Sigma). Ten randomly taken images were obtained for each experiment ($n = 3$) by using an Axioplan photomicroscope (×40 objective) equipped with an Axiocam digital camera (Zeiss). Apoptosis rate was determined as the percentage of cells with fragmented nuclei. The results are presented as mean ± SD. Statistical analysis was performed using paired Student's *t*-test, and results were considered significant at $P < 0.05$.

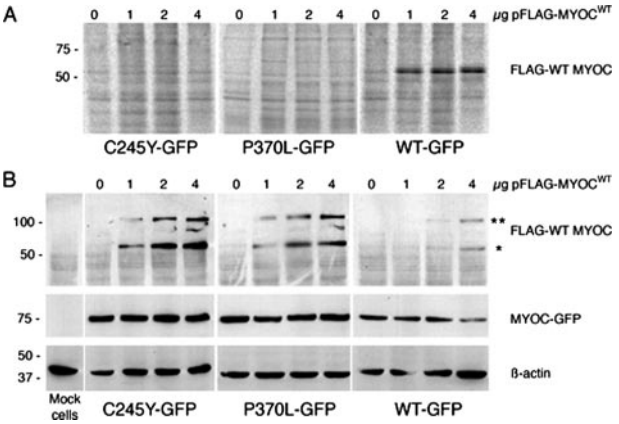

Figure 1. Heteromeric complexes of mutant and WT MYOC are not secreted and form detergent-insoluble aggregates. **A:** CHO cells stably expressing either mutant (C245Y, P370L) or WT MYOC-GFP were transfected with increasing amounts of pFLAG-MYOC^{WT} for 2 days in culture media containing 25 μCi/ml [^{35}S]cysteine and [^{35}S]methionine. The culture media were immunoprecipitated with anti-FLAG antibody, the samples resolved by 10% SDS-PAGE, and analyzed by phosphorimaging. **B:** Same material as in **A**. Cells were lysed in buffer containing 0.5% Triton X-100 and detergent-insoluble fractions were analyzed for FLAG, GFP, and β-actin by Western blotting. *Monomeric FLAG-WT MYOC, and **heteromeric FLAG-WT MYOC/MYOC-GFP complexes. The staining for GFP and β-actin served as loading control.

Results

Heteromeric Complexes of WT and Mutant MYOC Form Rough ER-Derived Russell Bodies

Recently, it has been shown that WT and mutant MYOCs form heteromeric protein complexes that are insoluble in Triton X-100.[30,31] Such detergent-insoluble MYOC aggregates cannot be secreted by the cells.[30,31] In the present work, we generated CHO-K1 and HEK293 cells stably expressing C-terminal GFP-tagged WT or mutant MYOC to initially verify the effect of an additional transient expression of FLAG-tagged WT MYOC on the solubility and secretion of the formed MYOC complexes. In previous studies, it was shown that MYOC tagged with GFP was secreted with a similar efficiency as MYOC without any tag.[30,44] We found that FLAG-WT MYOC transiently expressed in cells already stably expressing either C245Y or P370L MYOC-GFP fusion protein was not secreted as indicated by its absence in the culture medium (Figure 1A). Furthermore, we observed that it formed Triton X-100-insoluble complexes with mutant MYOC in a dose-dependent manner (Figure 1B). In addition, by Western blotting under reducing conditions, both monomeric (FLAG-tagged WT MYOC only) and heteromeric (GFP-tagged mutant MYOC and FLAG-tagged WT MYOC) forms were observed (Figure 1B). Cells co-expressing WT MYOC-GFP and FLAG-WT MYOC served as a reference (Figure 1, A and B). Thus, our cell culture system represents a suitable expression model to study the subcellular distribution of homomeric WT/WT and POAG-causing heteromeric mutant/WT MYOC complexes.

By confocal double immunofluorescence, both WT MYOC-GFP and FLAG-WT MYOC expressed in HEK293 cells displayed an overlapping, reticular staining pattern in the cytoplasm (Figure 2A). However, in cells co-ex-

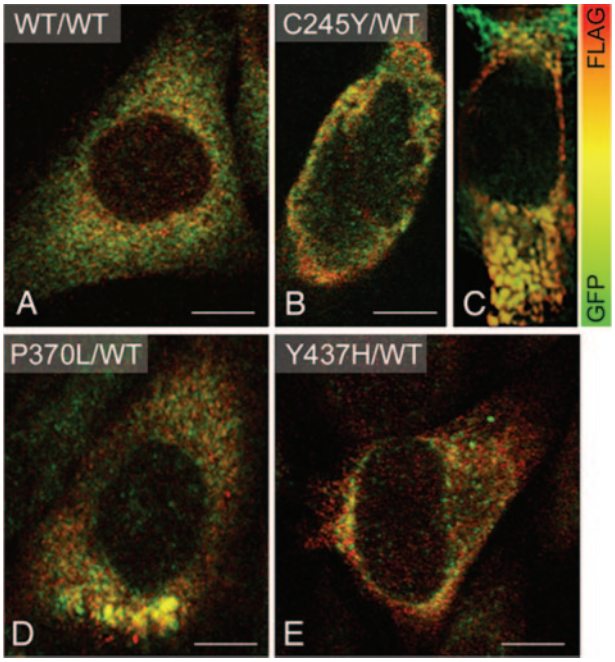

Figure 2. Co-expression of mutant and WT MYOC results in intracellular aggregate formation. **A:** Merged double-confocal immunofluorescence images of HEK293 cells expressing WT MYOC-GFP (green) and FLAG-WT MYOC (red) shows overlapping MYOC distribution as indicated by the orange-yellow color. MYOC aggregates are undetectable. **B** and **C:** C245Y- and WT MYOC-expressing cells exhibit distinct cytoplasmic aggregates composed of both mutant and WT MYOC as indicated by the orange-yellow color. Distinct cytoplasmic aggregates of varying sizes are also observed in P370L and WT MYOC-expressing (**D**) or Y437H-expressing and WT MYOC-expressing cells (**E**). Scale bars = 5 μm.

pressing mutant MYOC-GFP and FLAG-WT MYOC, additional distinct cytoplasmic aggregates of varying sizes composed of both mutant and WT MYOC fluorescent signals were observed (Figure 2, B–E). By transmission electron microscopy, the lumen of the rough ER cisternae in HEK293 cells co-expressing WT MYOC-GFP and FLAG-WT MYOC was narrow (Figure 3A). In contrast, ribosome-covered ER in HEK293 cells co-expressing C245Y MYOC-GFP and FLAG-WT MYOC showed a greatly expanded lumen (Figure 3, B and C; asterisks) representative of Russell bodies.[45,46] Rough ER cisternae with narrow lumen were observed next to the dilated ones (Figure 3B, arrowheads). This represents a classic finding because Russell body formation involves only part of the rough ER.[45,46] By immunoperoxidase electron microscopy, the Russell bodies were positive for FLAG-WT MYOC (Figure 3, D and E). Because the studied cells were clonally expressing the ER-retained C245Y MYOC-GFP (data not shown), this indicated that both C245Y and WT MYOC accumulated in the ER and induced the formation of Russell bodies. Similar results were obtained with P370L MYOC-GFP and FLAG-WT MYOC co-expressing cells (data not shown). In pulse-chase experiments using the proteasome inhibitor MG132, no evidence for proteasomal degradation of mutant and WT MYOC was obtained (Figure 4). Most probably, the detergent-insoluble MYOC aggregates cannot be retrotranslocated from the lumen of the ER to its cytosolic side. The observed ultrastructural changes were limited to the rough ER, with the nuclear envelope, the vesiculotubular clusters of the pre-Golgi intermediates, and the Golgi cisternal stack appearing normal (Figure 3C). Misfolded proteins have been detected in pre-Golgi intermediates and may cause its expansion.[47–50] We also detected mutant and WT MYOC in the pre-Golgi intermediates by confocal double immunofluorescence using the anti-ERGIC-53 antibody[51] as a marker for this structure (Figure 3, F and G). Although Russell bodies were detectable in the cytoplasm, none were observed in the ERGIC-53-positive elements (Figure 3E), which is in agreement with the ultrastructural findings (Figure 3C).

Myocilin-Induced Russell Bodies Cause ER Stress and Apoptosis

Intracellular accumulation of aggregated proteins often leads to an unfolded protein response and apoptotic cell death.[52–54] We analyzed by Western blotting the expression of BiP, the phosphorylated form of ER-localized eukaryotic initiation factor (eIF)-2α kinase (PERK) and caspase 12 as indicators of ER stress and unfolded protein responses. To achieve optimal solubilization of the proteins under investigation, RIPA buffer containing 1% Nonidet P-40 and 0.25% sodium deoxycholate instead of 0.5% Triton X-100 was used. Transient expression of FLAG-WT MYOC in HEK293 cells stably expressing C245Y or P370L MYOC-GFP resulted in the up-regulation of both BiP and PERK (Figure 5). Furthermore, caspase 12 activation, as indicated by the cleavage of the 60-kd pro-caspase 12 into its active 30- to 40-kd fragments, was observed in mutant/WT MYOC co-expressing cells (Figure 5). The activation of caspase 12 could not be observed in cells co-expressing WT/WT MYOC (Figure 5). Mock-transfected cells treated with dithiothreitol, to trigger nonspecific protein misfolding in the ER, served as a positive control for ER stress induction. Cells exhibited an increase in BiP and PERK expression and caspase 12 activation similar to mutant/WT MYOC-expressing cells (Figure 5). Next we studied the apoptosis mediators CHOP/GADD153 and caspase 3. In cells co-expressing mutant and WT MYOC or only mutant MYOC, both CHOP/GADD153 and active caspase 3 proteins were easily detectable, as in dithiothreitol-treated mock-transfected cells (Figure 5). In contrast, no increase in CHOP/GADD153 and active caspase 3 proteins was detected in WT/WT MYOC-expressing cells (Figure 5). To estimate the rate of apoptosis, immunofluorescence for MYOC and Hoechst 332518 DNA staining were combined. By double immunofluorescence, cells co-expressing mutant MYOC-GFP and FLAG-WT MYOC were unequivocally identified. Nuclear fragmentation visualized by DNA staining was taken as evidence for apoptosis. In Figure 6A, several HEK293 cells co-expressing C245Y MYOC-GFP and FLAG-WT MYOC can be seen as indicated by the orange-yellow color in the merged image. As expected, cells expressing only C245Y MYOC-GFP (green color) were also observed. Figure 6B shows the corresponding DNA-stained image demonstrating nuclear fragmentation in cells co-express-

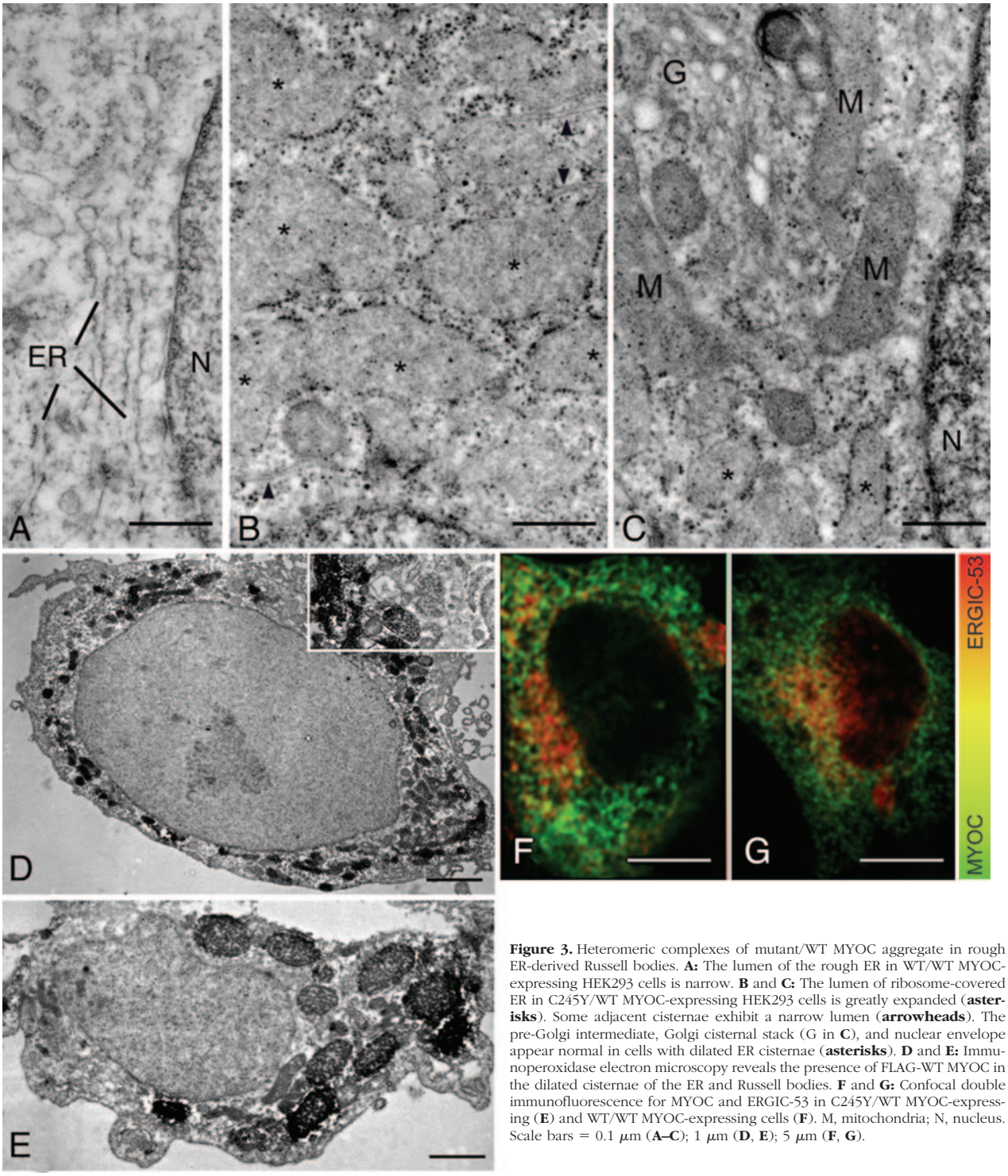

Figure 3. Heteromeric complexes of mutant/WT MYOC aggregate in rough ER-derived Russell bodies. **A:** The lumen of the rough ER in WT/WT MYOC-expressing HEK293 cells is narrow. **B** and **C:** The lumen of ribosome-covered ER in C245Y/WT MYOC-expressing HEK293 cells is greatly expanded (**asterisks**). Some adjacent cisternae exhibit a narrow lumen (**arrowheads**). The pre-Golgi intermediate, Golgi cisternal stack (G in **C**), and nuclear envelope appear normal in cells with dilated ER cisternae (**asterisks**). **D** and **E:** Immunoperoxidase electron microscopy reveals the presence of FLAG-WT MYOC in the dilated cisternae of the ER and Russell bodies. **F** and **G:** Confocal double immunofluorescence for MYOC and ERGIC-53 in C245Y/WT MYOC-expressing (**E**) and WT/WT MYOC-expressing cells (**F**). M, mitochondria; N, nucleus. Scale bars = 0.1 μm (**A–C**); 1 μm (**D**, **E**); 5 μm (**F**, **G**).

ing C245Y and WT MYOC. A low apoptosis rate was found for cells expressing WT MYOC when examined up to 5 days after transfection (Figure 6C). Only a slight increase in apoptosis rate was found for cells expressing only C245Y MYOC. However, a significant and time-dependent increase of the apoptosis rate was observed for cells co-expressing C245Y and WT MYOC (Figure 6C). At day 5 after transfection, the apoptosis rate of mutant/WT MYOC-expressing cells (C245Y/WT, 27.7 ± 2.4%; P370L/WT, 21.2 ± 2.1%; Y437H/WT, 27 ± 4%) was significantly higher ($P < 0.05$, paired Student's *t*-test) than for WT/WT MYOC-expressing cells (8.8 ± 1.7%) (Figure 6D). However, the increase was insignificant for G364V/WT cells (25.3 ± 10.6%). The increase in apoptosis rate was only observed for the studied POAG-causing mutant MYOC and not for the nondisease-causing polymorphism. This became evident when the POAG-causing R422C MYOC was compared with the nondisease-caus-

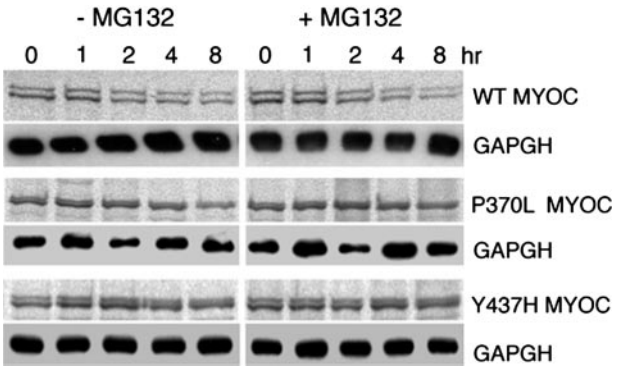

Figure 4. Turnover of WT and mutant MYOC-GFP is not influenced by proteasome inhibition. Autoradiogram of metabolically labeled and immunoprecipitated WT, P370L, and Y437H MYOC chased in the presence of 10 μmol/L MG132. Identical results were obtained for HTM cells (shown here) as well as HEK293 and CHO cells (not shown). Western blotting of GAPDH in soluble cell lysates served as loading control.

ing R422H MYOC polymorphism (Figure 6D). R422C MYOC showed a higher apoptosis rate (19.8 ± 4.2%) than the R422H polymorphism (10.2 ± 3.1%). The latter was in the range of the apoptosis rate of WT MYOC-expressing cells.

Discussion

Perturbation or blockage of aqueous humor outflow leading to elevated IOP is one of the strongest known risk factors of glaucoma.[4,55,56] This causes chronic

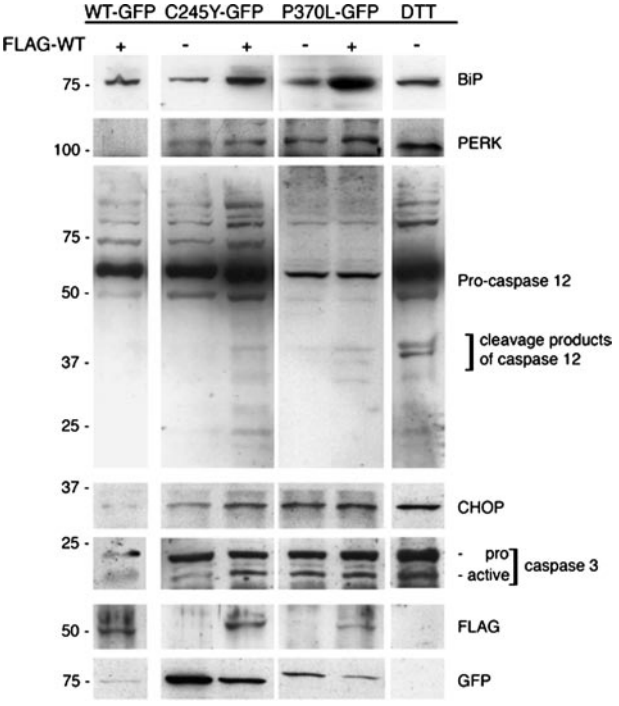

Figure 5. Heteromeric mutant/WT MYOC aggregates up-regulate unfolded protein response components. RIPA soluble lysates of WT/WT, C245Y/WT, and P370L/WT MYOC-expressing HEK293 cells were subjected to Western blotting for BiP, PERK, caspase 12, CHOP/GADD153, and caspase 3. The staining for FLAG and GFP demonstrates WT and mutant MYOC expression in these cells. Dithiothreitol-treated mock-transfected cells served as positive control for ER stress induction.

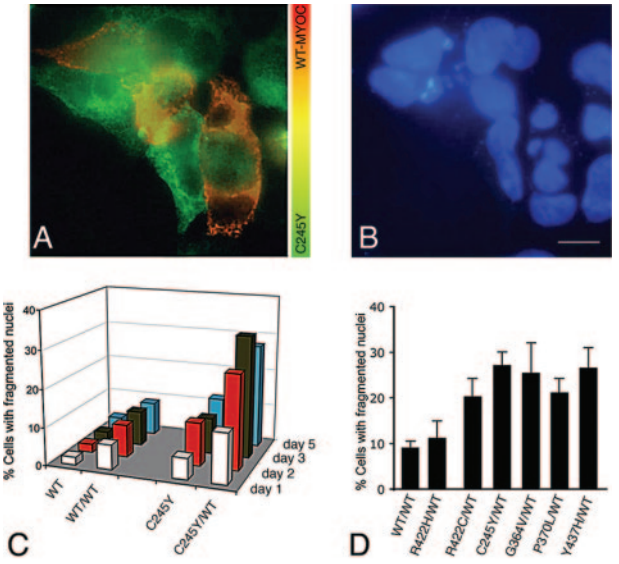

Figure 6. Heteromeric mutant/WT MYOC aggregates induce apoptosis. **A:** HEK293 cells stably expressing only C245Y MYOC-GFP appear in green whereas those co-expressing the mutant and the FLAG-WT MYOC can be identified by their orange-yellow color. **B:** The some cluster of cells as shown in **A** but stained by Hoechst 332518 DNA stain. The C245Y MYOC-GFP and FLAG-WT MYOC co-expressing cells exhibit fragmented nuclei **C:** Apoptosis rate was highest in C245Y/WT-expressing cells when compared with WT, WT/WT, or C245Y MYOC-expressing cells and increased with time after transfection. **D:** Apoptosis rate of different mutant/WT MYOC-expressing cells at day 5 after pFLAG-MYOC^{WT} transfection.

progressive damage to the retinal ganglion cells and results in irreversible loss of bilateral vision. From genetic studies, it has become apparent that *MYOC* gene mutations play a critical role in the manifestation of high IOP-associated POAG.[57–59] It is known that most POAG-causing mutants of MYOC, unlike WT MYOC, are misfolded and retained intracellularly, resulting in blockade of its secretion.[23–27,30,60] The impeded secretion of aggregated MYOC has been proposed to cause alterations of the extracellular matrix along the TM outflow pathway and to obstruct aqueous humor outflow.[3,4] However, the underlying molecular and cellular mechanisms through which mutant MYOC protein exerts its effect on the outflow drainage are mainly unknown. In an attempt to obtain further insight into the POAG pathogenesis, we have investigated the effects of heteromeric WT/mutant MYOC aggregates formed in cell cultures. The formation of heteromeric complexes between mutant and WT MYOC has been recognized as the basis of the pathological gain-of-function mechanism.[25,30,31] The C245Y, P370L, and Y437H MYOCs studied here cause severe juvenile-onset POAG.[11,61,62] We found that the detergent-insoluble, secretion-incompetent MYOC aggregates were retained in the lumen of the ER, caused the dilatation of parts of the rough ER, and resulted in ultrastructural changes characteristic of Russell bodies. We obtained no evidence for proteasomal degradation of ER-retained mutant C245Y, P370L, and Y437H MYOC aggregates. Apparently, the insoluble MYOC aggregates could not be retrotranslocated from the lumen of the ER to its cytosolic side and thus were not accessible for

proteasomal degradation in the cytosol. However, a robust ER stress response was induced by the MYOC aggregates in the ER lumen, resulting in apoptotic cell death. These data indicate that apoptosis may be a major pathogenetic factor for the development and progression of MYOC-caused POAG.

The folding state of glycoproteins in the ER is monitored by a protein quality control machinery.[63–66] Glycoproteins failing to fold properly will be retained in the ER and either be stored in this locale or become retrotranslocated and degraded by the ubiquitin-proteasome system.[45,67–69] The process involving retrotranslocation and proteasomal degradation of misfolded proteins is called ER-associated protein degradation (ERAD).[45,67–69] Thus, protein misfolding is the cause of a large spectrum of diseases as diverse as cystic fibrosis, α-1-antitrypsin deficiency, renal diabetes insipidus, congenital hypothyroid goiter, osteogenesis imperfecta, Parkinson's disease, and Alzheimer's disease, to name a few.[70–73] Incorrectly folded proteins retrotranslocated to the cytosol can induce the formation of inclusion bodies when the capacity of the ubiquitin-proteasome system is exhausted.[74,75] On the other hand, misfolded secretory proteins may form insoluble aggregates in the lumen of the ER, so-called Russell bodies.[45,50,76,77] In the classic meaning, Russell bodies are dilated rough ER cisternae containing aggregated, secretion-incompetent immunoglobulins that can neither be retrotranslocated nor be degraded by the ubiquitin-proteasome system. However, Russell bodies can be caused by other types of misfolded proteins and in nonlymphoid cell types.[50,70,78–81] Our electron microscopic findings are the first to demonstrate that detergent-insoluble, heteromeric aggregates formed by WT and various mutant MYOCs induce the formation of Russell bodies. This advances previous double-immunofluorescence data on ER retention of WT and Q368X or P370L MYOCs expressed in human TM cells.[26,30] In addition, we detected MYOC in pre-Golgi intermediates as indicated by its co-localization with ERGIC-53.[82] However, Russell bodies were not detectable in pre-Golgi intermediates as was also reported for cells expressing aberrant Ig light chains.[50,76,77] The presence of various types of misfolded glycoproteins in the pre-Golgi intermediates[47–50,83] is in agreement with its function as a protein quality control checkpoint.[84–87] Altogether, the present results show that aggregates formed by WT and mutant MYOC result in Russell body formation, a structural hallmark of ER storage diseases.

Accumulation of misfolded glycoproteins in the ER can result in ER stress and possibly in cell death.[52,53] This effect may be particularly pronounced when the misfolded glycoprotein cannot undergo ERAD[69] as is the situation when Russell bodies are formed because of mutant Ig[77] or mutant MYOC (present study). The mutant C245Y, P370L, or Y437H MYOC seems not to be degraded by the proteasome as we demonstrated in pulse-chase experiments in the presence of the proteasome inhibitor MG 132. As a consequence of the accumulation of mutant MYOC in Russell bodies, elevated levels of unfolded protein response components such as BiP, PERK, and CHOP/GADD153 as well as the activation of caspases 12 and 3 are observed. As a result, cells eventually undergo apoptosis, which represents the molecular pathway of cell damage elicited by mutant disease-causing MYOC but not nondisease-causing polymorphism (Figure 7).

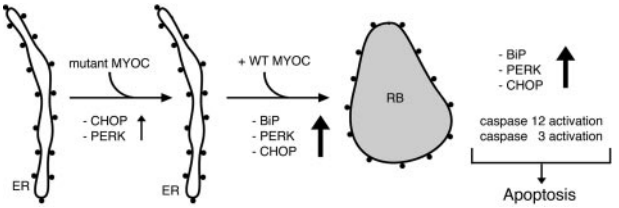

Figure 7. Summary of the proposed mechanism of mutant MYOC-caused apoptotic cell death. In cells expressing the ER-retained mutant MYOC only, PERK and CHOP are weakly induced. However, in cells co-expressing Russell body (RB)-forming, detergent-insoluble heteromeric aggregates of mutant and WT MYOC, BiP, PERK, and CHOP are strongly induced. In addition, activation of caspases 12 and 3 occurs. Eventually, the induction of unfolded protein response components and apoptosis mediators results in apoptotic cell death.

Although the present data were obtained in cell culture models, they obviously have implications for the pathogenesis of MYOC-caused POAG. We propose that the changes caused by the accumulation of aggregates formed by heteromeric complexes of WT and mutant MYOC also occur *in situ* in the TM cells in glaucoma patients. A progressive loss of TM cells by apoptosis should result in a progressive diminution of the phagocytotic capacity of the remaining TM cell population to clean the outflow drainage. This eventually results in humor outflow obstruction and elevated IOP. In support of our proposal are the electron microscopic findings from biopsies of nontreated MYOC-caused glaucoma patients showing a reduction of TM cells as well as thickened trabeculae and accumulation of sheath-derived plaques and of melanin.[36,39,40] The present data point to an important pathogenetic role of mutant MYOC and Russell body formation in the development of elevated IOP in POAG.

Acknowledgments

We thank T.D. Nguyen (San Francisco, CA) for providing immortalized HTM cells that were originally established by the late J.R. Polansky; H.P. Hauri (Basel, Switzerland) for providing the ERGIC-53 monoclonal antibody; and Charlotte Remé (Zurich, Switzerland) for helpful comments and suggestions.

References

1. Shields MB, Ritch R, Krupin T: Classification of the Glaucoma. Edited by R Ritch, MB Shields, T Krupin. Philadelphia, Mosby, 1996, pp 717–725
2. Quigley HA: Number of people with glaucoma worldwide. Br J Ophthalmol 1996, 80:389–393
3. Tamm ER: Myocilin and glaucoma: facts and ideas. Prog Retin Eye Res 2002, 21:395–428
4. Tan JC, Peters DM, Kaufman PL: Recent developments in understanding the pathophysiology of elevated intraocular pressure. Curr Opin Ophthalmol 2006, 17:168–174

5. Grierson I, Hogg P: The proliferative and migratory activities of trabecular meshwork cells. Prog Retin Eye Res 1995, 15:33–67
6. Acott TS, Westcott M, Passo MS, van Buskirk EM: Trabecular meshwork glycosaminoglycans in human and cynomolgus monkey eye. Invest Ophthalmol Vis Sci 1985, 26:1320–1329
7. Buller C, Johnson DH, Tschumper RC: Human trabecular meshwork phagocytosis. Observations in an organ culture system. Invest Ophthalmol Vis Sci 1990, 31:2156–2163
8. Rao PV, Deng P, Maddala R, Epstein DL, Li CY, Shimokawa H: Expression of dominant negative Rho-binding domain of Rho-kinase in organ cultured human eye anterior segments increases aqueous humor outflow. Mol Vis 2005, 11:288–297
9. Santas AJ, Bahler C, Peterson JA, Filla MS, Kaufman PL, Tamm ER, Johnson DH, Peters DM: Effect of heparin II domain of fibronectin on aqueous outflow in cultured anterior segments of human eyes. Invest Ophthalmol Vis Sci 2003, 44:4796–4804
10. Clark AF, Brotchie D, Read AT, Hellberg P, English-Wright S, Pang IH, Ethier CR, Grierson I: Dexamethasone alters F-actin architecture and promotes cross-linked actin network formation in human trabecular meshwork tissues. Cell Motil Cytoskeleton 2005, 60:83–95
11. Stone EM, Fingert JH, Alward LM, Nguyen TD, Polansky JR, Sunden SL, Nishimura D, Clark AF, Nystuen A, Nichols BE, Mackey DA, Ritch R, Kalenak JW: Identification of a gene that causes primary open angle glaucoma. Science 1997, 275:668–670
12. Alward WL, Fingert JH, Coote MA, Johnson AT, Lerner SF, Junqua D, Durcan FJ, McCartney PJ, Mackey DA, Sheffield VC, Stone EM: Clinical features associated with mutations in the chromosome 1 open-angle glaucoma gene (GLC1A). N Engl J Med 1998, 338:1022–1027
13. Swiderski RE, Ross JL, Fingert JH, Clark AF, Alward WL, Stone EM, Sheffield VC: Localization of MYOC transcripts in human eye and optic nerve by in situ hybridization. Invest Ophthalmol Vis Sci 2000, 41:3420–3428
14. Huang W, Jaroszewski J, Ortego J, Escribano J, Coca-Prados M: Expression of the TIGR gene in the iris, ciliary body, and trabecular meshwork of the human eye. Ophthalmic Genet 2000, 21:155–169
15. Karali A, Russell P, Stefani F, Tamm E: Localization of myocilin/trabecular meshwork-inducible glucocorticoid response protein in the human eye. Invest Ophthalmol Vis Sci 2000, 41:729–740
16. Tamm ER, Polansky JR: The TIGR/MYOC gene and glaucoma: opportunities for new understandings. J Glaucoma 2001, 10:S9–S12
17. Ueda J, Wentz-Hunter K, Yue BY: Distribution of myocilin and extracellular matrix components in the juxtacanalicular tissue of human eyes. Invest Ophthalmol Vis Sci 2002, 43:1068–1076
18. Fautsch MP, Vrabel AM, Johnson DH: The identification of myocilin-associated proteins in the human trabecular meshwork. Exp Eye Res 2006, 82:1046–1052
19. Gobeil S, Letartre L, Raymond V: Functional analysis of the glaucoma-causing TIGR/myocilin protein: integrity of amino-terminal coiled-coil regions and olfactomedin homology domain is essential for extracellular adhesion and secretion. Exp Eye Res 2006, 82:1017–1029
20. Whitmore AV, Libby RT, John SW: Glaucoma: thinking in new ways—a role for autonomous axonal self-destruction and other compartmentalized processes? Prog Retin Eye Res 2005, 24:639–662
21. Kim BS, Savinova OV, Reedy MV, Martin J, Lun Y, Gan L, Smith RS, Tomarev SI, John SW, Johnson RL: Targeted disruption of the myocilin gene (Myoc) suggests that human glaucoma-causing mutations are gain of function. Mol Cell Biol 2001, 21:7707–7713
22. Gould DB, Miceli-Libby L, Savinova OV, Torrado M, Tomarev SI, Smith RS, John SWM: Genetically increasing Myoc expression supports a necessary pathologic role of abnormal proteins in glaucoma. Mol Cell Biol 2004, 24:9019–9025
23. Zhou Z, Vollrath D: A cellular assay distinguishes normal and mutant TIGR/myocilin protein. Hum Mol Genet 1999, 8:2221–2228
24. Jacobson N, Andrews M, Shepard AR, Nishimura D, Searby C, Fingert JH, Hageman G, Mullins R, Davidson BL, Kwon YH, Alward WL, Stone EM, Clark AF, Sheffield VC: Non-secretion of mutant proteins of the glaucoma gene myocilin in cultured trabecular meshwork cells and in aqueous humor. Hum Mol Genet 2001, 10:117–125
25. Joe MK, Sohn S, Hur W, Moon Y, Choi YR, Kee C: Accumulation of mutant myocilins in ER leads to ER stress and potential cytotoxicity in human trabecular meshwork cells. Biochem Biophys Res Commun 2003, 312:592–600
26. Liu Y, Vollrath D: Reversal of mutant myocilin non-secretion and cell killing: implications for glaucoma. Hum Mol Genet 2004, 13:1193–1204
27. Vollrath D, Liu YH: Temperature sensitive secretion of mutant myocilins. Exp Eye Res 2006, 82:1030–1036
28. Morissette J, Clepet C, Moisan S, Dubois S, Winstall E, Vermeeren D, Nguyen TD, Polansky JR, Cote G, Anctil JL, Amyot M, Plante M, Falardeau P, Raymond V: Homozygotes carrying an autosomal dominant TIGR mutation do not manifest glaucoma. Nat Genet 1998, 19:319–321
29. Lam DS, Leung YF, Chua JK, Baum L, Fan DS, Choy KW, Pang CP: Truncations in the TIGR gene in individuals with and without primary open-angle glaucoma. Invest Ophthalmol Vis Sci 2000, 41:1386–1391
30. Sohn S, Hur W, Joe MK, Kim JH, Lee ZW, Ha HS, Kee C: Expression of wild-type and truncated myocilins in trabecular meshwork cells: their subcellular localizations and cytotoxicities. Invest Ophthalmol Vis Sci 2002, 43:3680–3685
31. Gobeil S, Rodrigue MA, Moisan S, Nguyen TD, Polansky JR, Morissette J, Raymond V: Intracellular sequestration of hetero-oligomers formed by wild-type and glaucoma-causing myocilin mutants. Invest Ophthalmol Vis Sci 2004, 45:3560–3567
32. Shirato S, Murphy CG, Bloom E, Franse-Carman L, Maglio MT, Polansky JR, Alvarado JA: Kinetics of phagocytosis in trabecular meshwork cells. Flow cytometry and morphometry. Invest Ophthalmol Vis Sci 1989, 30:2499–2511
33. Schlotzer-Schrehardt U, Naumann GO: Trabecular meshwork in pseudoexfoliation syndrome with and without open-angle glaucoma. A morphometric, ultrastructural study. Invest Ophthalmol Vis Sci 1995, 36:1750–1764
34. Matsumoto Y, Johnson DH: Dexamethasone decreases phagocytosis by human trabecular meshwork cells in situ. Invest Ophthalmol Vis Sci 1997, 38:1902–1907
35. Lütjen-Drecoll E, Shimizu T, Rohrbach M, Rohen JW: Quantitative analysis of 'plaque material' in the inner- and outer wall of Schlemm's canal in normal- and glaucomatous eyes. Exp Eye Res 1986, 42:443–455
36. Rohen JW, Lütjen-Drecoll E, Flugel C, Meyer M, Grierson I: Ultrastructure of the trabecular meshwork in untreated cases of primary open-angle glaucoma (POAG). Exp Eye Res 1993, 56:683–692
37. Gottanka J, Flugel-Koch C, Martus P, Johnson DH, Lütjen-Drecoll E: Correlation of pseudoexfoliative material and optic nerve damage in pseudoexfoliation syndrome. Invest Ophthalmol Vis Sci 1997, 38:2435–2446
38. Lütjen-Drecoll E: Functional morphology of the trabecular meshwork in primate eyes. Prog Retin Eye Res 1999, 18:91–119
39. Cracknell KP, Grierson I, Hogg P, Majekodunmi AA, Watson P, Marmion V: Melanin in the trabecular meshwork is associated with age, POAG but not Latanoprost treatment. A masked morphometric study. Exp Eye Res 2006, 82:986–993
40. Alvarado J, Murphy C, Juster R: Trabecular meshwork cellularity in primary open-angle glaucoma and nonglaucomatous normals. Ophthalmology 1984, 91:564–579
41. Polansky JR, Weinreb RN, Baxter JD, Alvarado J: Human trabecular cells. I. Establishment in tissue culture and growth characteristics. Invest Ophthalmol Vis Sci 1979, 18:1043–1049
42. Brown WJ, Farquhar MG: Immunoperoxidase methods for the localization of antigens in cultured cells and tissue sections by electron microscopy. Methods Cell Biol 1989, 31:553–569
43. Yam GHF, Zuber C, Roth J: A synthetic chaperone corrects the trafficking defect and disease phenotype in a protein misfolding disorder. FASEB J 2005, 19:12–18
44. Mertts M, Garfield S, Tanemoto K, Tomarev SI: Identification of the region in the N-terminal domain responsible for the cytoplasmic localization of Myoc/Tigr and its association with microtubules. Lab Invest 1999, 79:1237–1245
45. Kopito RR, Sitia R: Aggresomes and Russell bodies. Symptoms of cellular indigestion? EMBO Rep 2000, 1:225–231
46. Pavelka M, Roth J: Functional Ultrastructure: An Atlas of Tissue Biology and Pathology. Wien, Springer Medicine, 2005
47. Raposo G, van Santen HM, Leijendekker R, Geuze HJ, Ploegh HL: Misfolded major histocompatibility complex class I molecules accumulate in an expanded ER-Golgi intermediate compartment. J Cell Biol 1995, 131:1403–1419
48. Gilbert A, Jadot M, Leontieva E, Wattiaux-De Coninck S, Wattiaux R:

Delta F508 CFTR localizes in the endoplasmic reticulum-Golgi intermediate compartment in cystic fibrosis cells. Exp Cell Res 1998, 242:144–152
49. Zuber C, Fan JY, Guhl B, Roth J: Misfolded proinsulin accumulates in expanded pre-Golgi intermediates and endoplasmic reticulum subdomains in pancreatic beta cells of Akita mice. FASEB J 2004, 18:917–919
50. Mattioli L, Anelli T, Fagioli C, Tacchetti C, Sitia R, Valetti C: ER storage diseases: a role for ERGIC-53 in controlling the formation and shape of Russell bodies. J Cell Sci 2006, 119:2532–2541
51. Schindler R, Itin C, Zerial M, Lottspeich F, Hauri HP: ERGIC-53, a membrane protein of the ER-Golgi intermediate compartment, carries an ER retention motif. Eur J Cell Biol 1993, 61:1–9
52. Kaufman RJ: Orchestrating the unfolded protein response in health and disease. J Clin Invest 2002, 110:1389–1398
53. Nadanaka S, Yoshida H, Kano F, Murata M, Mori K: Activation of mammalian unfolded protein response is compatible with the quality control system operating in the endoplasmic reticulum. Mol Biol Cell 2004, 15:2537–2548
54. Schröder M, Kaufman RJ: ER stress and the unfolded protein response. Mutat Res 2005, 569:29–63
55. Sommer A, Tielsch JM, Katz J, Quigley HA, Gottsch JD, Javitt J, Singh K: Relationship between intraocular pressure and primary open angle glaucoma among white and black Americans. The Baltimore Eye Survey. Arch Ophthalmol 1991, 109:1090–1095
56. Shields MB: Textbook of Glaucoma. Baltimore, Williams & Wilkins, 1992
57. Wiggs JL, Allingham RR, Vollrath D, Jones KH, De La Paz M, Kern J, Patterson K, Babb VL, Del Bono EA, Broomer BW, Pericak-Vance MA, Haines JL: Prevalence of mutations in TIGR/myocilin in patients with adult and juvenile primary open-angle glaucoma. Am J Hum Genet 1998, 63:1549–1552
58. Fingert JH, Heon E, Liebmann JM, Yamamoto T, Craig JE, Rait J, Kawase K, Hoh ST, Buys YM, Dickinson J, Hockey RR, Williams-Lyn D, Trope G, Kitazawa Y, Ritch R, Mackey DA, Alward WL, Sheffield VC, Stone EM: Analysis of myocilin mutations in 1703 glaucoma patients from five different populations. Hum Mol Genet 1999, 8:899–905
59. Faucher MP, Anctil JL, Rodrigue MA, Duchesne A, Bergeron D, Blondeau P, Cote G, Dubois S, Bergeron J, Arseneault R, Morissette J, Raymond V, Quebec Glaucoma Network: Founder TIGR/myocilin mutations for glaucoma in the Quebec population. Hum Mol Genet 2002, 11:2077–2090
60. Caballero M, Borras T: Inefficient processing of an olfactomedin-deficient myocilin mutant: potential physiological relevance to glaucoma. Biochem Biophys Res Commun 2001, 282:662–670
61. Adam MF, Belmouden A, Binisti P, Brezin AP, Valtot F, Bechetoille A, Dascotte JC, Copin B, Gomez L, Chaventre A, Bach JF, Garchon HJ: Recurrent mutations in a single exon encoding the evolutionarily conserved olfactomedin-homology domain of TIGR in familial open-angle glaucoma. Hum Mol Genet 1997, 6:2091–2097
62. Fan BJ, Leung DYL, Wang DY, Gobeil S, Raymond V, Tam POS, Lam DSC, Pang CP: Novel myocilin mutation in a Chinese family with juvenile-onset open-angle glaucoma. Arch Ophthalmol 2006, 124:102–106
63. Roth J: Protein N-glycosylation along the secretory pathway: relationship to organelle topography and function, protein quality control and cell interactions. Chem Rev 2002, 102:285–303
64. Ellgaard L, Helenius A: Quality control in the endoplasmic reticulum. Nat Rev Mol Cell Biol 2003, 4:181–191
65. Trombetta ES, Parodi AJ: Quality control and protein folding in the secretory pathway. Annu Rev Cell Dev Biol 2003, 19:649–676
66. Sitia R, Braakman I: Quality control in the endoplasmic reticulum protein factory. Nature 2003, 426:891–894
67. Ahner A, Brodsky JL: Checkpoints in ER-associated degradation: excuse me, which way to the proteasome? Trends Cell Biol 2004, 14:474–478
68. Hirsch C, Jarosch E, Sommer T, Wolf DH: Endoplasmic reticulum-associated protein degradation—one model fits all? Biochim Biophys Acta 2004, 1695:208–216
69. Meusser B, Hirsch C, Jarosch E, Sommer T: ERAD: the long road to destruction. Nat Cell Biol 2005, 7:766–772
70. Kim PS, Arvan P: Endocrinopathies in the family of endoplasmic reticulum (ER) storage diseases: disorders of protein trafficking and the role of ER molecular chaperones. Endocr Rev 1998, 19:173–202
71. Aridor M, Hannan LA: Traffic jams II: an update of diseases of intracellular transport. Traffic 2002, 3:781–790
72. Ross CA, Poirier MA: Protein aggregation and neurodegenerative disease. Nat Med 2004, 10:S10–S17
73. Carrell RW: Cell toxicity and conformational disease. Trends Cell Biol 2005, 15:574–580
74. Johnston JA, Ward CL, Kopito RR: Aggresomes: a cellular response to misfolded proteins. J Cell Biol 1998, 143:1883–1898
75. Kopito RR: Aggresomes, inclusion bodies and protein aggregation. Trends Cell Biol 2000, 10:524–530
76. Alanen A, Pira U, Lassila O, Roth J, Franklin RM: Mott cells are plasma cells defective in immunoglobulin secretion. Eur J Immunol 1985, 15:235–242
77. Valetti C, Grossi CE, Milstein C, Sitia R: Russell bodies: a general response of secretory cells to synthesis of a mutant immunoglobulin which can neither exit from, nor be degraded in the endoplasmic reticulum. J Cell Biol 1991, 115:983–994
78. Palade GE: Intracisternal granules in the exocrine cells of the pancreas. J Biophys Biochem Cytol 1956, 2:417–422
79. Tooze J, Kern HF, Fuller SD, Howell KE: Condensation-sorting events in the rough endoplasmic reticulum of exocrine pancreatic cells. J Cell Biol 1989, 109:35–50
80. Lomas DA, Evans DL, Finch JT, Carrell RW: The mechanism of Z alpha 1-antitrypsin accumulation in the liver. Nature 1992, 357:605–607
81. Medeiros-Neto G, Kim PS, Yoo SE, Vono J, Targovnik HM, Camargo R, Hossain SA, Arvan P: Congenital hypothyroid goiter with deficient thyroglobulin. Identification of an endoplasmic reticulum storage disease with induction of molecular chaperones. J Clin Invest 1996, 98:2838–2844
82. Hauri HP, Kappeler F, Andersson H, Appenzeller C: ERGIC-53 and traffic in the secretory pathway. J Cell Sci 2000, 113:587–596
83. Hsu VW, Yuan LC, Nuchtern JG, Lippincott-Schwartz J, Hammerling GJ, Klausner RD: A recycling pathway between the endoplasmic reticulum and the Golgi apparatus for retention of unassembled MHC class I molecules. Nature 1991, 352:441–444
84. Lucocq JM, Brada D, Roth J: Immunolocalization of the oligosaccharide trimming enzyme glucosidase II. J Cell Biol 1986, 102:2137–2146
85. Zuber C, Fan JY, Guhl B, Parodi A, Fessler JH, Parker C, Roth J: Immunolocalization of UDP-glucose:glycoprotein glucosyltransferase indicates involvement of pre-Golgi intermediates in protein quality control. Proc Natl Acad Sci USA 2001, 98:10710–10715
86. Taxis C, Vogel F, Wolf DH: ER-Golgi traffic is a prerequisite for efficient ER degradation. Mol Biol Cell 2002, 13:1806–1818
87. Vashist S, Ng DT: Misfolded proteins are sorted by a sequential checkpoint mechanism of ER quality control. J Cell Biol 2004, 165:41–52